2538–2546 Nucleic Acids Research, 1994, Vol. 22, No. 13

Structural elements of *rpsO* mRNA involved in the modulation of translational initiation and regulation of *E.coli* ribosomal protein S15

Claude Philippe, Lionel Bénard[1], Flore Eyermann, Claire Cachia[2], Stanislav V.Kirillov[3], Claude Portier[1], Bernard Ehresmann and Chantal Ehresmann*

UPR 9002 du CNRS, Institut de Biologie Moléculaire et Cellulaire,15 rue René Descartes, 67084-Strasbourg cedex, [1]Institut de Biologie Physico-Chimique,13 rue Pierre et Marie Curie, 75005-Paris, [2]Laboratoire de Biophysique, Faculté de Pharmacie, 7 boulevard Jeanne d'Arc, 21000 Dijon, France and [3]Laboratory of Protein Biosynthesis, Nuclear Physic Institut, 188350 Gatchina, St Petersbourg district, Russia

Received April 8, 1994; Revised and Accepted May 31, 1994

ABSTRACT

Previous experiments showed that S15 inhibits its own translation by binding to its mRNA in a region overlapping the ribosome loading site. This binding was postulated to stabilize a pseudoknot structure that exists in equilibrium with two stem-loops and to trap the ribosome on its mRNA loading site in a transitory state. In this study, we investigated the effect of mutations in the translational operator on: the binding of protein S15, the formation of the 30S/mRNA/ $tRNA_f^{Met}$ ternary initiation complex, the ability of S15 to inhibit the formation of this ternary complex. The results were compared to *in vivo* expression and repression rates. The results show that (1) the pseudoknot is required for S15 recognition and translational control; (2) mRNA and 16S rRNA efficiently compete for S15 binding and 16S rRNA suppresses the ability of S15 to inhibit the formation of the active ternary complex; (3) the ribosome binds more efficiently to the pseudoknot than to the stem-loop; (4) sequences located between nucleotides 12 to 47 of the S15 coding phase enhances the efficiency of ribosome binding *in vitro*; this is correlated with enhanced *in vivo* expression and regulation rates.

INTRODUCTION

In the cell, the synthesis of ribosomal components should obey to a double requirement: co-ordinating the synthesis of individual ribosomal RNAs and proteins, and balancing ribosome synthesis rate against the growth conditions. In *E.coli*, the synthesis of most r-proteins is regulated at the translational level (reviewed in 1). Almost all regulatory r-proteins are rRNA 'primary' binding proteins which bind directly and individually to the rRNA during the early stages of ribosomal assembly. Since regulatory r-proteins recognize specific RNA targets, auto regulation most likely involves recognition of common structural features on their mRNA and rRNA target sites (2). Indeed, strong sequence and secondary structure similarities exist between the mRNA and rRNA binding sites of protein S8 (3–4) and some resemblance was detected in the case of proteins L1 (5) and L10 (6). The binding of the regulatory r-protein to its mRNA target site may block translational initiation by three possible ways: (a) the protein binds to its mRNA in a region which overlaps with the ribosomal binding site, thereby preventing ribosome binding by direct competition; (b) the binding of the protein induces a conformational change in the mRNA which masks the ribosome entry site; (c) the bound r-protein blocks a step in the translational initiation pathway subsequent to the binding of the 30S subunit to the mRNA, preventing the formation of the first peptide bond (proposed as 'entrapment model' by Draper (7). So far, none of the investigated mechanisms seem to involve simple direct competition (1).

The translational autogenous control of the *rpsO* gene, coding for r-protein S15 was evidenced by Portier *et al.* (8). The regulatory site was genetically located in the leader of the mRNA overlapping the ribosome loading site and the first codons. Using structure probing experiments (9), we showed that the regulatory region folds into three distinct domains that are able to adopt either a stem-loop or a pseudoknot conformation (Fig. 1). It was postulated that these two conformations are in dynamic equilibrium and that the binding of S15 stabilizes the pseudoknot form (Fig. 1). Site-directed mutagenesis suggested that the formation of the pseudoknot is required for an efficient auto control (8–10). More recently, we showed that S15 does not prevent the ribosome to bind to its initiation loading site *in vitro*, but stabilizes the binary 30S/mRNA complex and traps the ribosome in a transient complex unable to form an active initiation complex with the initiator tRNA (11).

In the present study, we investigated the role of the pseudoknot in modulating S15 recognition and ribosome binding. This was

*To whom correspondence should be addressed

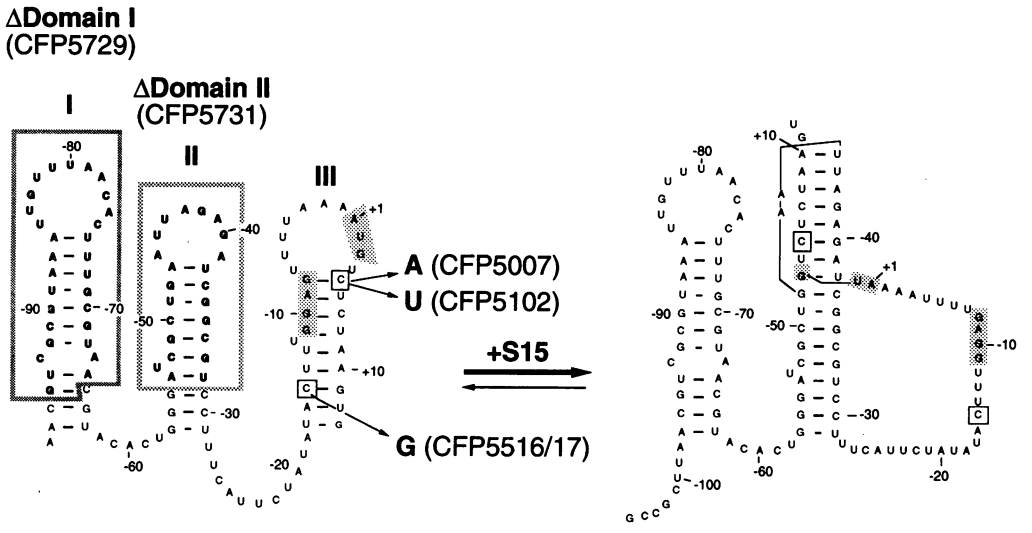

Figure 1. The postulated equilibrium between the two alternative secondary structures adopted by the wild-type mRNA. The equilibrium is shifted to the pseudoknot conformation as a consequence of S15 binding. The structure is from Philippe *et al.* (9). In CFP5516/17 a weak helix may pair AUCUUA(−25) to UGAGGUU(−13), with A(−9) bulging out (9). The Shine-Dalgarno sequence and the initiation codon are shadowed in both structures. The studied mutations are indicated by arrows. Point mutations are boxed.

correlated with the ability of S15 to inhibit *In vItro* the formation of the active ternary 30S/mRNA/tRNA$_f^{Met}$ initiation complex, and with expression and repression rate *in vivo*. New *rpsO-lacZ* fusions were also constructed, that eliminates additional sequences at both 5′ and 3′ and displace the point of fusion downstream. The results indicate that proximal *rpsO* sequences are crucial for optimal translation and repression.

MATERIAL AND METHODS

Strain and plasmid construction

Most plasmids used in this study were described in a previous work (8, 9, 11). A new translational fusion was constructed between *rpsO* and *lacZ* by fusing the proximal part of *rpsO* till the *Pst*I site to the distal part of *lacZ* (fusion *rpsO−lacZ2*, Fig. 2). Fragment *Hpa*I−*Pst*I of the *rpsO* gene was inserted in M13mp8 cut by *Sma*I and *Pst*I. Two new sites (*Hpa*I and *Sal*I) were created just downstream of the transcription start and after the 16th codon of S15, respectively (11) (Fig. 2). Two derivatives of the fusion *rpsO−lacZ2* were constructed. The first one, *rpsO−lacZD3*, was obtained by removing the fragment *Sca*I−*Sal*I (Fig.2) after cleavage by *Sal*I, treatment with Mung bean nuclease, subsequent cleavage by *Sca*I, ligation and transformation. In the second derivative, *rpsO−lacZ*Δ4, the fragment *Sal*I−*Hind*III was removed after cleavage and filling of the protruding ends by Klenow enzyme. The two shortened derivatives were screened on Xgal plates after ligation and transformation into JM101 *rec*A strain. An in frame blue fusion of each type was isolated and sequenced. Transfer of the fusions into phage lambda, lysogenisation of the strain AB5311 and β-galactosidase activity were as previously described (8). The *Hpa*I−*Sal*I fragment was inserted into the Bluescribe vector and used to obtain RNA transcripts containing only a few additional nucleotides, as previously described (11).

Preparation of the biological material

RNAs were obtained by *in vitro* transcription of Bluescribe plasmids with RNA polymerase from phage T7, as previously described (9, 11). Plasmid arising from the first construction were linearised either by *Hind*III (for filter binding assays) or by *Pvu*II (for toeprinting experiments) and those arising from the second construction by *Sal*I or *Hind*III (Fig. 2). Uniformly labelled RNA was prepared by adding [α-^{32}P] UTP in the transcription medium, and purified by 10 % polyacrylamide (0.5 % bis-acrylamide)/8 M urea gel electrophoresis. The RNA fragments were renatured prior use by incubation at 42°C for 10 min in the appropriate buffer and cooled on ice. Protein S15 was fractionated according to (12). *E.coli* 30S subunits were fractionated from tight couples according to a procedure adapted from (13) and incubated for 15 min at 37°C prior use. The 16S rRNA fragment (nucleotides 578 to 756) containing the binding site of protein S15 was prepared according to (14).

Filter binding assays

Complexes were formed by incubating about 40,000 cpm of uniformly labelled RNA (≈ 0.1 nM) with increasing concentration of S15 (from 5 nM to 5 μM) at 4°C for 20 min in buffer A (50 mM-Tris acetate (pH 7.5), 20 mM-Mg acetate, 270 mM-KCl, 5 mM-dithiothreitol) in the presence of 0.02 %-bovine serum albumin. The samples were filtered on nitro-cellulose filters (Millipore GS, 0,22 μm) soaked in buffer A before use. The filters were washed with 300 μl of buffer A, dried and counted for radioactivity. Aspecific retention of RNA (about 10 %) was measured by filtrating the reaction mixture in the absence of S15. Competition assays contained a constant concentration of the uniformly labelled 16S rRNA fragment (≈ 0.1 nM, about 40,000 cpm) and protein S15 (0.7 μM). Unlabeled wild-type or variant competitor mRNAs were varied from 5 nM to 5 μM.

Table 1. Comparison of the *in vivo* expression and repression levels in the different translational *rpsO−lacZ* fusions.

Plasmids / Strains	pBR322 (control)	pBP111 (S15)	Repression ratio
CFP5312 *(rpsO-lacZ1)*	109 ≠ 4	21 ± 2	5
CFP5313 *(rpsO-lacZ2)*	856 ± 50	39 ± 3	22
CFP5314 *(rpsO-lacZΔ3)*	115 ± 6	11 ± 2.6	10
CFP5315 *(rpsO-lacZΔ4)*	654 ± 181	26 ± 3.5	26

The *in vivo* effect was analysed by measuring the β-galactosidase activity (expressed in Miller units) of the translational fusions carried by a bacteriophage l. The corresponding lysogenic strains were tranformed by plasmids pBR322 (control) and pBP111 (overproducing S15 in *trans*). The values measured in the absence and in the presence of S15 in *trans* are indicated and the 'repression ratio' is expressed by the ratio between these two values.

Inhibition analysis of the translational initiation complex (toeprinting)

The formation of the ternary 30S/mRNA/$tRNA_f^{Met}$ complex and toeprinting experiments were adapted from (15). Standard reactions contained 200 nM 30S subunits, 24 nM mRNA, 2 mM non-acylated initiator tRNA and S15 at the indicated concentration, in 10 μl of 20 mM-Tris-acetate (pH 7.5), 60 mM-NH_4Cl, 10 mM-Mg acetate, 3 mM-β-mercaptoethanol. Incubation was for 15 min at 37°C when non specified. Reverse transcription was conducted with 0.5 unit of AMV reverse transcriptase (Life Sciences) for 15 min at 37°C, using as primers labelled oligonucleotides complementary to nucleotides 81 to 96 and 38 to 50 for RNAs derived from *rpsO−lacZ1* and *rpsO−LacZ2*, respectively. The reactions were stopped by the addition of 10 μl of loading buffer and heating to 90°C for 2 min. The mixture was loaded on a 10 % polyacrylamide/8 M urea gel and submitted to electrophoresis at 1200 V for 2 h.

RESULTS

Description of the experimental system

The conformation of the wild-type mRNA and of the mutants shown in Fig. 1 was previously studied (9). These mRNA fragments all contained additional sequences at their 5′ extremity, corresponding to 39 nucleotides upstream of the natural initiation transcription site and 32 plasmid nucleotides resulting from the construction. A new fusion was constructed (*rpsO−lacZ2*), in which the 5′ additional nucleotides were removed and in which the fusion point was displaced till the middle of the *rpsO* mRNA (Fig. 2). In the following, WT1 and WT2 will refer to RNAs resulting from the *rpsO−lacZ1* and *rpsO−lacZ2* fusions, respectively. From chemical probing experiments, we showed that the conformation of the leader region is unaffected by the

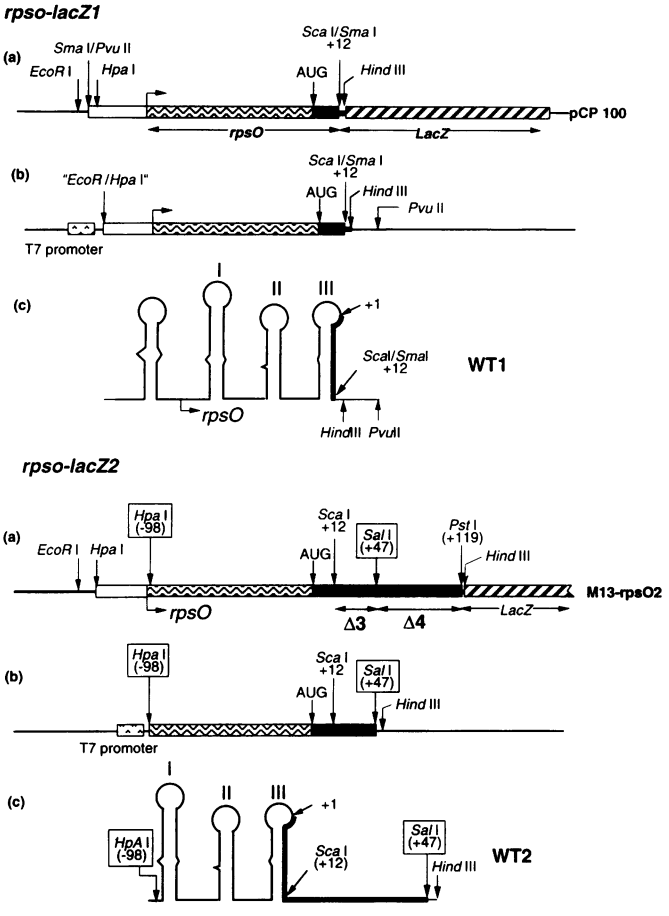

Figure 2. Comparison between the two rpsO−lacZ fusions and correspondIng RNA transcripts. (**a**) DNA plasmids used to transfer fusion into phage lambda *prior* lysogenization. (**b**) Bluescribe plasmids used as template for *in vitro* transcription. (**c**) Synthesised RNA transcripts. Coding phases from *rpsO* and *lacZ* are represented by black and crossed bars, respectively. The *rpsO* transcription start is indicated by a broken arrow. Strategic restriction sites are shown and the newly created sites are boxed.

deletion of the additional sequences and the displacement of the fusion (results not shown). Most mutant RNAs used in this study were obtained from the *rpsO−lac Z1* construct. However, the G-15 mutation was introduced in both fusions (CFP5516 and CFP5517 referring to RNAs obtained from *rpsO−lacZ1* and *rpsO−lacZ2*, respectively).

The long fusion rpsO−lacZ2 is more efficiently expressed and repressed than the short one

The level of β-galactosidase expression in the short and long translational fusions was measured in the absence and in the presence of S15 in *trans* (Table 1). The ratio between these two values is a measure of the 'repression ratio'. Unexpectedly, the level of β-galactosidase in the absence of S15 in *trans*, which is about 110 units for the fusion *rpsO−lacZ1*, raises to about 850 units for the fusion *rpsO−lacZ2*. Moreover, the repression ratio obtained upon addition of S15 in *trans* increases from 5 in the short fusion, to 22 in the long fusion. Thus, displacing the point of fusion 100 nucleotides downstream in the coding sequence of *rpsO* increases the level of translational efficiency

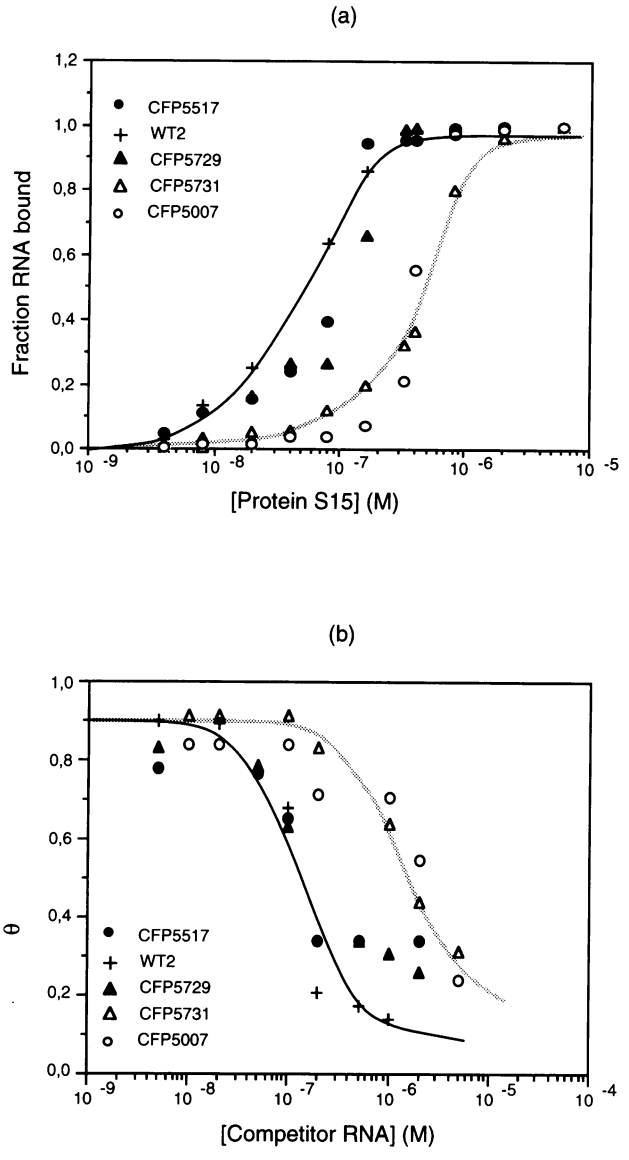

Figure 3. Interaction between S15 and wild-type and mutant mRNA transcripts. (**a**) Titration experiments showing the binding of S15 with wild-type and mutant mRNA transcripts. Dissociation constants were evaluated as the concentration of S15 necessary to obtain half-saturation, assuming that complex formation obeys to a simple bimolecular equilibrium. This treatment assumes that $[P_{free}] = [P_{total}]$; this condition is fulfilled in the assay since the RNA concentration is negligible compared to the concentration of total protein. (**b**) Competition between unlabeled mRNA transcripts and the labelled 16S rRNA fragment for S15 binding. The symbols are as indicated; the solid and dashed lines show the experimental curves of WT2 and CFP5731, respectively.

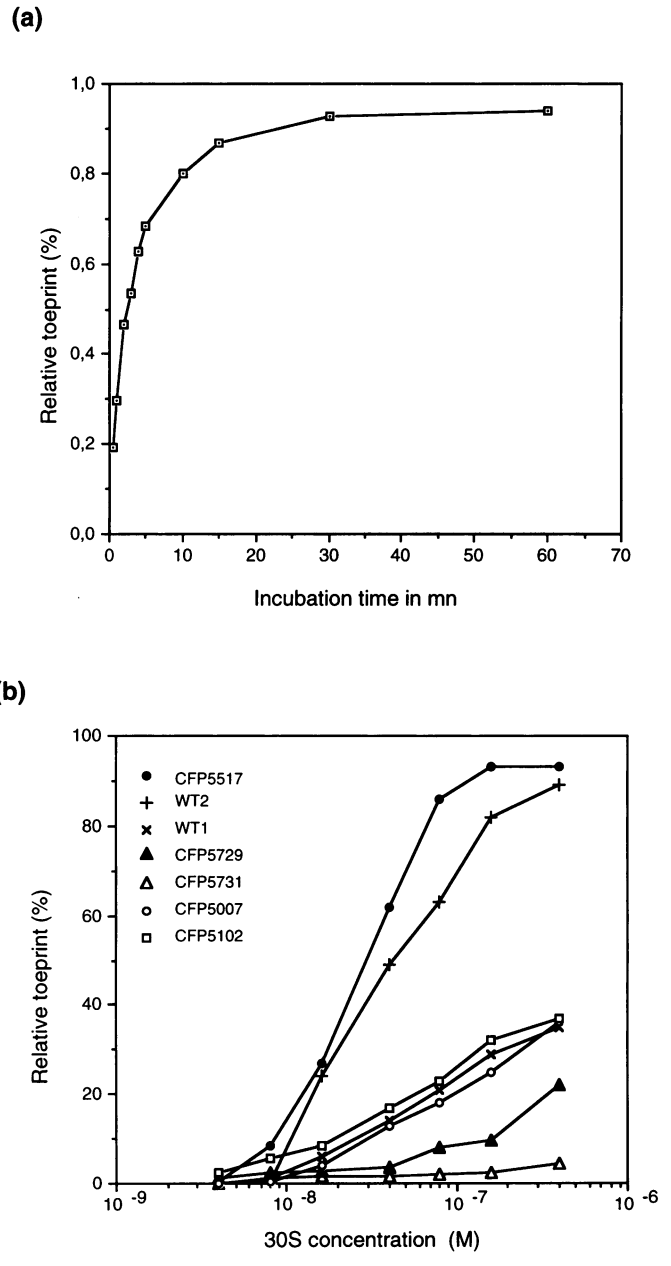

Figure 4. Formation of the ternary 30S/mRNA/$tRNA_f^{Met}$ complex. (**a**) Kinetics of formation of the wild-type ternary complex. The ternary complex was formed at 37°C with 24 nM WT2 mRNA, 200 nM 30S subunit and 2 μM initiator tRNA. (**b**) Formation of the various ternary complexes as a function of 30S subunit concentration. Toeprinting experiments were done as in (a) in the presence of increasing concentrations of 30S subunits (from 4 nM to 400 nM). Relative toeprinting (toeprint band over 5′ ends + toeprint) were calculated by scanning of the gel with the Bio-Imager Analyzer BAS 2000 (Fuji). The relative toeprinting intensities were plotted as a function of incubation time.

(measured in the absence of S15 in *trans*) by a factor of 7 to 8 and the repression ratio by a factor of 4 to 5.

To further investigate the role of downstream sequences in expression and repression, two deletions were created, removing either the proximal (*rpsO−lacZΔ3*) or the distal part (*rpsO−lacZΔ4*) of the *rpsO* sequence present in fusion *rpsO−lacZ2* (Fig. 2). The distal deletion (*rpsO−lacZΔ4*) has no significant effect on the translation and repression efficiency (Table 1). On the opposite, the proximal deletion (*rpsO−lacZΔ3*) reduces both expression and repression levels. The expression level is pulled down to the same level as that of *rpsO−lac Z1*, while the repression ratio is lowered by a factor of ≈2. These observations suggest that nucleotides 12 to 47 are involved in translational and regulatory efficiency.

Protein S15 discriminates the mRNA variants

Nitro-cellulose filter binding assays have been widely used to study RNA−protein interactions (e.g. 3, 16−19). They provide a reliable comparative analysis of the binding strengths of various

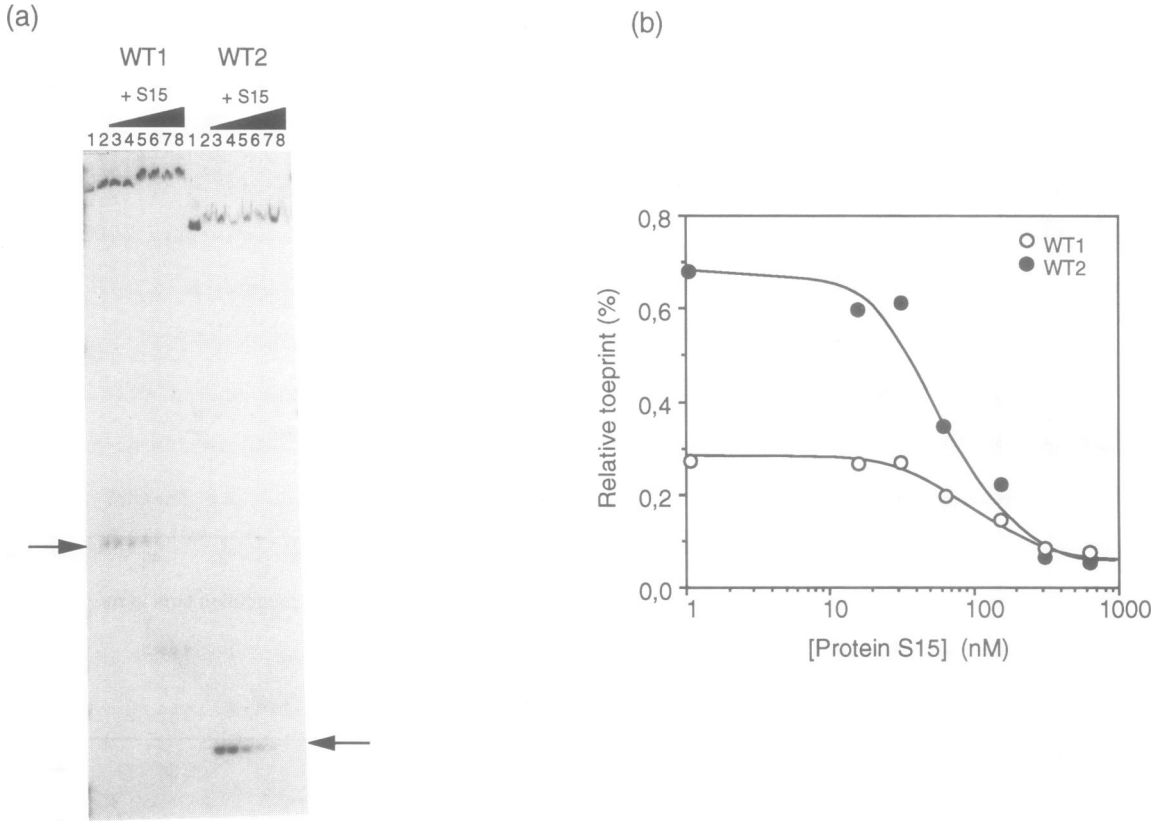

Figure 5. Inhibitory effect of S15 on the formation of the ternary 30S/WT mRNA/$tRNA_f^{Met}$ complex. (**a**) Toeprinting experiments showing the formation of the ternary complex with WT1 and WT2 upon addition of increasing concentrations of protein S15. Experiments were conducted under standard conditions: control minus tRNA (lane 1); plus tRNA (lane 2); plus S15 (15, 30, 60, 150, 300 and 600 nM; lanes 3 to 8, respectively). The position of the toeprint is indicated by arrows. (**b**) Relative toeprint intensity as a function of S15 concentration. Data are from the gel shown in (a).

RNAs for a given protein. The apparent association constant for the wild-type mRNA and each mutant was estimated by titrating a low and constant concentration of labelled RNA with increasing concentrations of S15. The apparent association constant was also estimated for a 16S rRNA fragment (nucleotides 578 to 756), containing the binding site of S15 (14). Measurements were repeated in 2 to 5 independent experiments. Typical titration curves are shown in figure 3a.

Our results indicate that S15 recognizes its binding site on 16S rRNA and on the two mRNA constructs (WT1 or WT2) with a similar apparent Kd (30 ± 15 nM and 53 ± 20 nM, respectively). A Scatchard analysis indicates that the wild-type mRNA binds S15 with a 1:1 stoichiometry (results not shown). Controls made in parallel indicate that the *X.laevis* 5S rRNA shows some weak binding (Kd > 10 μM) and that ribosomal protein S8 is unable to bind the wild-type RNA fragment in the same range of concentration (results not shown). It turns out that the mutant mRNAs can be divided into two classes. The first one contains CFP5516/17 and CFP5729 which still bind S15 with a binding affinity similar to that of the wild-type mRNA, in the range of experimental error. Earlier results show that the deletion of domain I (CFP5759) does not affect the stem-loop/pseudoknot equilibrium and that the G-15 mutation (CFP5516/17), by destabilizing stem-loop III, leads to a constitutive pseudoknot (9). The second class corresponds to CFP5731, CFP5007 and CFP5102, showing a significant drop of their relative binding strength (by a factor of 4 to 10). Remarkably, these mutants are all affected in their capacity to form the pseudoknot (9). The deletion of domain II (CFP5731) prevents its formation and leads to a constitutive stem-loop III, while the C5 substitution destabilizes both stem-loop and pseudoknot structures, with a less pronounced effect with the C to U mutation which still allows a G-U pair. Therefore, there is a direct correlation between the capacity of the mRNA to form the pseudoknot and the affinity of S15.

The mRNA transcripts were also tested for their capacity to compete with the 16S rRNA fragment. The results show that the wild-type mRNA and the 16S rRNA fragment do compete for S15 binding (Fig. 3b). They also indicate that the tested mutants can be subdivided into the same two classes already defined above: the first one including CFP5517 and CFP5529, competing with 16S rRNA as well as the wild-type RNA; the second one including CFP5007 and CFP5731, showing a reduced competition strength. In summary, the binding affinity of S15 for the different mutants, together with their ability to compete with the 16S rRNA fragment, depends on the capacity of the RNA to form a specific pseudoknot (Table 2). Moreover, those mutations that reduce the binding and competition strengths also decrease the repression rate *in vivo* (Table 2).

The ribosomal 30S subunit binds to mRNA variants with different rate constants

The ability of the wild-type and mutant mRNA fragments to form the 30S ternary 30S/mRNA/$tRNA_f^{Met}$ initiation complex was

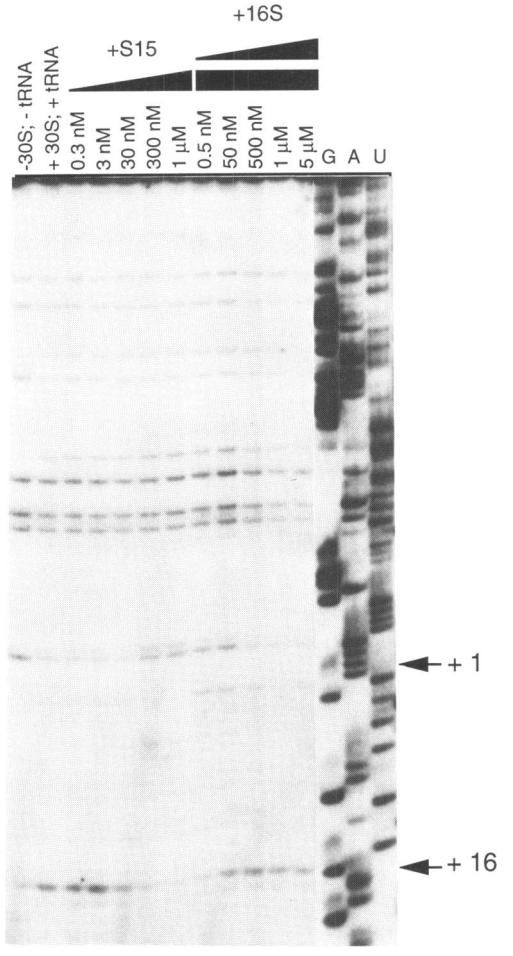

Figure 6. The 16S rRNA fragment as an anti repressor. Toeprinting experiments were conducted under standard conditions with WT2. The concentration of S15 and of the 16S rRNA fragment was varied as indicated; the rRNA fragment was added in the presence of 1 μM S15. G, A and U are sequencing lanes. The position of the toeprint is indicated.

compared by the use of the toeprinting technique devised by Hartz *et al.* (15). This approach is based on the fact that the ternary complex is able to block reverse transcription from a DNA primer (annealed to the mRNA downstream of the ribosome loading site), resulting in a stop at position +16 (A of the AUG initiation codon being 1), called toeprint. First, we studied the kinetics of formation of the ternary initiation complex under standard conditions. Results show that the reaction is completed after 15 min incubation (Fig. 4a). In agreement with others (20–21), we found that the ternary complex is stable for hours (results not shown).

The respective effect of the two RNA constructions and of the mutations on the formation of the ternary complex was compared by measuring the yield of toeprint as a function of 30S concentration (Fig. 4b). Since the formation of the ternary complex is almost irreversible, the observed differences reflect the association rate constant. Interestingly, we found that WT2 is able to form the ternary initiation complex with a higher rate constant than WT1 (Fig. 4b). The two C5 substitutions (CFP5007 and CFP5102) do not significantly alter the rate constant, as compared to WT1. Deletion of domain I (CFP5729) reduces the toeprinting strength and deletion of domain II (CFP5731) strongly inhibits ribosome binding. The effect of the C-15 to G substitution could only be tested in CFP5517, since a strong stop of reverse transcription at position +16 in CFP5516 prevents any correct interpretation of toeprinting experiments. This mutation does not impair the toeprinting strength and even appears to increase slightly the rate constant (as compared to WT2).

Effect of mutations on S15-induced inhibition of the ternary initiation complex

Previous results indicate that the binding of S15 stabilizes a pre-ternary initiation complex and prevents the formation of the active ternary 30S/mRNA/initiator tRNA complex (11). The ability of S15 to inhibit the formation of the active ternary complex was followed by the disappearance of the +16 toeprint in standard toeprinting experiments, using AMV reverse transcriptase. Note that the +10 toeprint, the signature of the trapped 30S subunit, is not visualised under the present conditions, since it is only detected by the use of Murine leukemia reverse transcriptase under sub-optimal conditions (11). The results show that the addition of increasing concentrations of S15 leads to a progressive reduction of the wild-type ternary complex, until a complete disappearance (Fig. 5a). As shown in Fig. 5, WT2 appears to be more sensitive to the titration effect of S15 than WT1. Half inhibition is obtained with WT1 and WT2 near a S15 concentration of 110 nM and 70 nM, respectively (Fig. 5b).

Since filter binding assays showed that there is a competition between the rRNA and mRNA fragments for S15 binding, it was expected that the addition of the rRNA fragment should derepress the formation of the ternary complex by displacing S15 from the mRNA. Indeed, the addition of increasing concentrations of rRNA, while keeping S15 at a constant concentration that inhibits the formation of the ternary complex, progressively restores the toeprint (Fig. 6).

The effect of addition of increasing amounts of S15 on the formation of the ternary complex was then tested with the various mRNA variants. In the case of CFP5729 and CFP5517, the toeprint progressively decreases in a range of S15 concentration similar to that observed for the wild-type RNA (Fig. 7). As for CFP5731 and CFP5007, the addition of S15 up to 1.5 mM has virtually no effect on the toeprint (Fig. 7). In the case of CFP5102, the toeprint appears to be sensitive to S15, but in a higher concentration range than for the wild-type RNA (Fig. 7). Our results show that mutations that do not affect S15 binding do not alter the capacity of S15 to inhibit the formation of the ternary complex. Conversely, S15 fails to inhibit the formation of the ternary complex in the case of mutations that decrease the affinity for S15.

DISCUSSION

The pseudoknot is required for S15 recognition and translational control

Previous results suggest that the translational operator exists as dynamic equilibrium between a stem-loop structure and a pseudoknot and that the latter is stabilized by S15 (9, 11). In this work we show that there is a correlation between the ability of the mRNA leader to adopt the pseudoknot conformation and its affinity for S15 (Table 2), suggesting that the pseudoknot is an essential structural element for S15 recognition. Our results are also supported by the fact that a C substitution at position −40 is able to compensate a G substitution at position +5 (10). The model also predicts that mutations that decrease the affinity

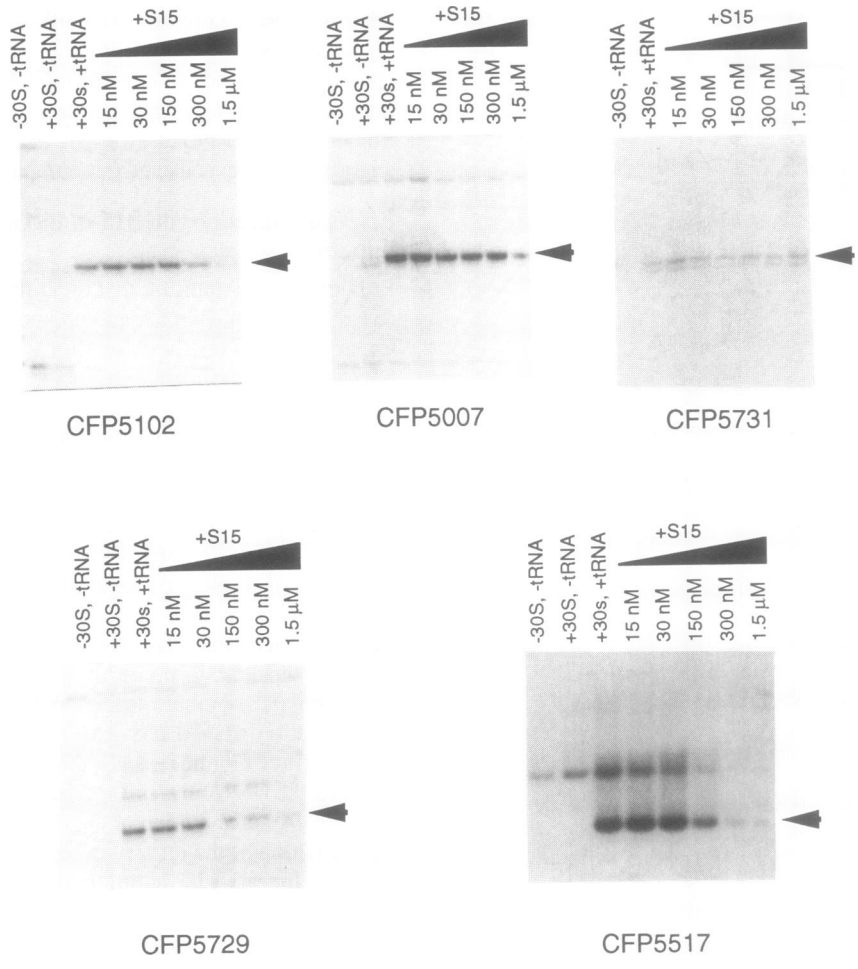

Figure 7. Effect of the mutations on the ability of S15 to inhibit the formation of the ternary complex. Toeprinting experiments were conducted under standard conditions with the various mRNA species. Arrows point to the stop of the reverse transcriptase at position +16. The concentration of S15 is varied between 15 nM to 1.5 µM as indicated.

for S15 reduce its ability to inhibit the formation of the active ternary 30S/mRNA/$tRNA_f^{Met}$ complex. This is exactly what is observed (Table 2). Furthermore, mutants that fail to prevent the formation of the ternary complex also fail to repress the expression *in vivo*. This double mutation that restores the capacity of the mRNA to form the pseudoknot also restore the *in vivo* control.

mRNA and rRNA compete for binding to S15

Interestingly, S15 recognizes its target site on mRNA and 16S rRNA with a similar binding affinity. Moreover, both rRNA and mRNA fragments compete for protein binding, as observed in the case of the L10-L12 complex (22) and of S4 (23). From these observations and taking into account the small size of S15, it appears that S15 most probably recognizes common structural features in both RNAs. However, no obvious similarities could be found between both mRNA and 16S rRNA binding sites. Recently, the GAAG sequence located at the 3′ edge of the pseudoknot in WT2 (nucleotides 16 to 19), showing a potential similarity with a sequence strongly conserved in the S15 rRNA binding site was proposed to be involved in S15 recognition (24). However, this sequence cannot be considered as a S15 determinant, since it is not present in WT1 which is recognized by S15 as well as WT2. If structural similarities exist between the two RNA binding sites, they should probably be found at the level of the tertiary structure (most likely in the pseudoknot conformation).

Furthermore, the addition of 16S rRNA was found to suppress the ability of S15 to inhibit the formation of the active ternary complex. This result strongly suggests that 16S rRNA acts as an anti-repressor by displacing the repressor from the mRNA, thus allowing the formation of an active ternary complex. The release of translational inhibition by the cognate rRNA or tRNA target was already observed in the case of S20 (25), L1 (26) and *E.coli* threonyl-tRNA synthetase (27). This repression/anti-repression mechanism allows to precisely regulate the synthesis rate of S15 to the intracellular concentration of 16S rRNA in a co-ordinated way.

How does the ribosome recognize its mRNA binding site?

The expression of a given gene is primarily controlled at the level of translational initiation. This is dependent upon both primary sequence and secondary structures of the translational initiation region (for reviews see 28–30). In the present case, the initiation region can adopt two alternative conformations in equilibrium (Fig. 1). Previous results showed that the ribosome can bind the

Table 2. Effect of mRNA mutations on the relative binding and competition strengths, on the intensity of toeprint and on the S15-dependent inhibition of the formation of the ternary 30S/mRNA/$tRNA_f^{Met}$ complex.

mRNA	Binding strength	Competition strength	RNA structure	Toeprinting strength	Expression level	S15-induced inhibition	Repression ratio
WT1	1	nd	(a) and (b)	++	1.0*	+	6.56-10*
CFP5729	0.6	0.5	(a) and (b)	+	0.8*	+	6.5-7.4*
CFP5516	0.7	nd	(b)	nd	0.6*	nd	8.5-8.6*
CFP5102	0.25	n.d.	other	++	7.2*	±	1.9*
CFP5007	0.1	0.05	other	++	7.3*	-	1.1*
CFP5731	0.1	0.05	(a)	±	1.25*	-	0.9-1.1*
WT2	1	1	(a) and (b)	+++	7.8	+	21
CFP5517	0.7	1	(b)	+++	nd	+	nd

The binding strength is expressed as the ratio of the dissociation association constant (Kd) measured for the wild-type mRNA over that measured for the mutant RNA. Kd values were obtained from saturation curves (see Fig. 3). The competition strength is expressed as the ratio of mutant to wild type mRNA concentrations required to provide a 50% competition value. The results are correlated with the capacity of the mRNA to adopt the stem-loop (a) or the pseudoknot (b) structure (from Philippe *et al.*, 1990). Note that the two C5 substitutions (CFP5102 and CFP5007) were shown to cause a destabilisation of the pseudoknot and of stem-loop III. In particular, the C to A change was found to induce the formation of alternative conformers in domain III. S15-induced inhibition refers to the formation of the ternary 30S/mRNA/$tRNA_f^{Met}$ complex. *In vivo* expression levels refer to the expression of β-galactosicase level in the absence of S15 in *trans* (in the presence of the control plasmid pBR322). They are expressed with respect to the value of WT1 (=1.0). The values marked with an asterisk are calculated from Table 3 and 5 of Portier *et al.* (8). Repression ratios are calculated as described in Table 1. Values marked with an asterisk are taken from Table 3 and 5 of (8). (n.d.) is not determined.

pseudoknot form and that this form is stabilized by S15 (11). The conversion of an inactive complex to a productive ternary initiation complex probably requires the unfolding of the pseudoknot. The bound S15 prevents this conversion and traps the ribosome in an inactive transitory stage. Therefore, mutations that alter the stem-loop/pseudoknot equilibrium or favour some alternative structure are expected to affect the translational initiation. Thus, we compared the effects of mutations on the efficiency to form the ternary complex *in vitro* (measured by the toeprinting strength) with the *in vivo* expression level in the absence of S15 in *trans* (Table 2). At first glance, there is no direct correlation between these *in vitro* and *in vivo* data. However, it should be reminded that the measured *in vivo* expression level is modulated by two different factors: the initiation efficiency and the repression caused by the endogenous copy of the *rpsO* gene.

The most dramatic effect on the toeprinting strength is caused by the deletion of domain II (CFP5731). The drop of initiation efficiency can be easily accounted by the sequestration of the Shine-Dalgarno sequence in a stable stem-loop structure, in agreement with previous observations that show that the mRNA secondary structure reduces the efficiency of translational initiation (30). However, this mutation does not significantly affect the *in vivo* expression level, while it results in a complete loss of regulation (Table 2). Therefore, this mutant displays a constitutive phenotype, that compensates for the reduced initiation efficiency. Conversely, mutating C5 (CFP5007 and CFP5102) does not affect the toeprinting strength, while the *in vivo* expression level is increased. These mutations were shown to destabilize both stem-loop III and pseudoknot, probably favouring a random coiled structure that is efficiently recognized by the ribosome. The increased expression level therefore directly reflects the loss of repression.

Interestingly, the C to G substitution at position −15 (CFP5516) that favours a constitutive pseudoknot conformation (9) shows a wild-type phenotype (Table 2). Toeprinting data conducted on this mutant (arising from the second construction) clearly show that the pseudoknot is quite efficiently recognized by the 30S subunit, probably refecting the fact that the Shine−Dalgarno sequence is fully accessible for ribosome binding. Moreover, footprinting experiments indicated that the bound S15 increases the accessibility of the Shine−Dalgarno sequence, in full agreement with the entrapment model (11). This is to parallel with results on the a operon mRNA, in which a pseudoknot stimulates 30S binding at low temperature while preventing subsequent formation of the proper ternary complex (21). In this case also, the regulatory protein S4 traps the mRNA in an inactive conformation (31).

The deletion of domain I (CFP5729) results in a slightly decreased expression level (with an unchanged repression efficiency). Surprisingly, it reduced the toeprinting strength, while it does not alter the conformational equilibrium. The reduction of the initiation efficiency is possibly related to the removal of a sequence located in the loop of hairpin I, analogous to a sequence that acts as a translational enhancer when located upstream of a gene (32).

Unexpectedly, displacing the point of fusion between *rpsO* and *lacZ* downstream in the S15 coding sequence (*rpsO−lacZ2* fusion) induces a strong increase of the toeprinting strength that is correlated with an enhanced *in vivo* expression rate. This effect is lost when the proximal region (nucleotides 12 to 47) is removed. Since the conformation of the leader is unchanged in both constructions, two possible explanations can be postulated: (1) the *lacZ* coding sequences fused near the AUG initiation codon in the first fusion negatively affects translation; (2) enhancer sequences are located in nucleotides 12 to 47. However, it should

be noted that the *lacZ* sequences are not present in the *in vitro* transcript WT2 but substituted by plasmid sequences. Since the toeprinting strength of WT1 is clearly reduced with respect to that of WT2 (which contains the *rpsO* sequences), the second hypothesis appears as a likely explanation. Noteworthy, the coding region corresponding to nucleotides 12 to 47 contains sequences which show some analogy with a region located downstream of the initiation codon, that have been postulated to act as translational enhancer (33–35). This point would merit further investigation. The increased expression level is accompanied by an increased repression ratio. This result can be correlated with the fact that the inhibition of the ternary initiation complex formation is more sensitive to the titration effect of S15 in WT2 than in WT1, thus supporting previous assumption that S15 and 30S subunit bind to the mRNA co-operatively (11). Also the fact that the efficiency of repression increases with the efficiency of translation is fully consistent with the entrapment mechanism. In the case of a competition mechanism, the increased affinity of the mRNA for the ribosome would have favour ribosome binding against S15 binding, resulting in a decreased repression efficiency.

ACKNOWLEDGEMENTS

We are indebted to V.I.Makhno and V.I.Katunin (Gatchina) for their help in preparing highly active 30S subunits. We thank P.Romby and C.Brunel for stimulating discussions. M.Grunberg-Manago (Paris) is thanked for her constant interest and support. This work is supported by grants from the Centre National de la Recherche Scientifique (UPR 9002 and UA1139) and from the Fondation de la Recherche Médicale (UPR 9002).

REFERENCES

1. Zengel, J.M. and Lindahl, L. *Prog. Nucl. Acids Res. and Mol. Biol.*, in press.
2. Nomura, M., Gourse, R. and Baughman, G. (1984). *Annu. Rev. Genet.* **53**, 73–117.
3. Gregory, R.J., Cahill, P.B.F., Thurlow, D.L. and Zimmermann, R.A. (1988) *J. Mol. Biol.* **204**, 295–307.
4. Ceretti, D.P., Mattheakis, L.C., Kearney, K.R., Vu, L. and Nomura, M. (1988). *J. Mol. Biol.* **204**, 309–329.
5. Kearney, K.R. and Nomura, M. (1987). *Mol. Gen. Genet.* **210**, 60–68.
6. Christensen, T., Johnsen, M., Fiil, N.P. and Friesen J.D. (1984). *EMBO J.* **3**, 1609–1612.
7. Draper, D.E. (1988). In—*Translational Regulation of Gene Expression*— (Ilan, J. ed.) Plenum Publishing, New York, pp 1–26.
8. Portier, C., Dondon, L. and Grunberg-Manago, M. (1990a). *J. Mol. Biol.* **211**, 407–414.
9. Philippe, C., Portier, C., Grunberg-Manago, M., Ebel, J. P., Ehresmann, B. and Ehresmann, C. (1990) *J. Mol. Biol.* **211**, 415–426.
10. Portier, C., Philippe, C., Dondon, J., Grunberg-Manago, M., Ebel, J.P., Ehresmann, B. and Ehresmann, C. (1990b). *Biochim. Biophys. Acta* **1050**, 328–336.
11. Philippe, C., Eyermann, F., Bénard, L., Portier, C., Ehresmann, B. and Ehresmann, C. (1993). *Proc. Natl. Acad. Sci. USA* **90**, 4394–4398.
12. Cachia, C., Flamion, P.J. and Schreiber, J.P. (1991). *Biochimie*, **73**, 607–610.
13. Makhno, V.I., Peshin, N.N., Semenkov, Yu. P. and Kirillov, S.V. (1988). *Molekulyarnaya Biologiya* **22**, 670–679.
14. Mougel, M., Philippe, P., Ebel, J.P., Ehresmann, B. and Ehresmann, C. (1988). *Nucleic Acids Res.* **16**, 2829–2839.
15. Hartz, D., McPheeters, D.S., Traut, R. and Gold, L. (1988). In *Methods of Enzymology* (Noller, H. F. and Moldave, K., eds), vol. **164**, pp. 419–425, Academic Press Inc., New York.
16. Deckman, I.C. and Draper, D.E. (1985). *Biochemistry* **24**, 7860–7865.
17. Baudin, F., Romaniuk, P., Romby, P., Brunel, C., Westhof, E., Ehresmann, B. and Ehresmann, C. (1991). *J. Mol. Biol.* **218**, 69–81.
18. Mougel, M., Allmang, C., Eyermann, F., Cachia, C., Ehresmann, B. and Ehresmann, C. (1993) *Eur. J. Biochem.* **215**, 787–792.
19. Draper, D.E., Deckman, I.C., and Vartikar, J.V. (1988). *Methods In Enzymology* 164, 203–220.
20. Gualerzi, C.O., Risuelo, G. and Pon, C. (1979). *J. Biol. Chem.* **254**, 44–49.
21. Spedding, G., Gluick, T. and Draper, D. (1993). *J. Mol. Biol.* **229**, 609–622.
22. Johnson, M., Christensen, T., Dennis, P.P. and Fiil, N.P. (1982) *EMBO J.* **8**, 999–1004.
23. Deckman, I. C. and Draper, D.E. (1987). *J. Mol. Biol.* **196**, 323–332.
24. Zwieb, C. (1992) *Nucleic Acids Res.* **20**, 4397–43.
25. Wirth, R., Kohles, V. and Böck, A. (1981) *Eur. J. Biochem.* **114**, 429–437.
26. Yates, J.L. and Nomura, M. (1981) *Cell* **24**, 243–249.
27. Moine, H., Romby, P., Springer, M., Grunberg-Manago, M., Ebel, J.P., Ehresmann, B. and Ehresmann, C. (1990). *J. Mol. Biol.* **216**, 299–310.
28. Hartz, D., McPheeters, D. and Gold, L. (1990) In *The Structure, Function and Evolution of Ribosomes* (Hill, W. ed.) Washington, DC:American Society for Microbiology, pp275–280.
29. McCarthy, J. E. G. and Gualerzi, C. (1990) *Trends Genet.* **6**, 78–85.
30. de Smit, M. H. and van Duin, J. (1990). *Prog. Nucl. Acids Res. Mol. Biol.* **38**, 1–35.
31. Spedding, G. and Draper, D.E. (1993) *Proc. Natl. Acad. Sci. USA* **90**, 4399–4403.
32. Olins, P.O. and Rangwala, J., (1989). *J. Biol. Chem.* **264**, 16973–16976.
33. Sprengart, M. L., Fatsher, H.P. and Fuchs, E. (1990). *Nucl. Acids Res.* **18**, 1719–1723.
34. Shean, C.S. and Gottesman, M.E. (1992). *Cell* **70**, 513–522.
35. Ito, K., Kawakami, K. and Nakamura, Y. (1993) *Proc. Natl. Acad. Sci. USA* **90**, 302–306.